

Climate response to volcanic forcing: Validation of climate sensitivity of a coupled atmosphere-ocean general circulation model

Tokuta Yokohata,^{1*} Seita Emori,^{1,2} Toru Nozawa¹
Yoko Tsushima², Tomo'o Ogura¹ and Masahide Kimoto³

¹National Institute for Environmental Studies

²Frontier Research Center for Global Change

²Center for Climate System Research

Submitted to *Science*, April 13, 2005

*To whom correspondence should be addressed; E-mail: yokohata.tokuta@nies.go.jp

Abstract

Two versions of a coupled atmosphere-ocean general circulation model with different climate sensitivities are tested on global cooling following the Pinatubo volcanic eruption to investigate the validity of high climate sensitivities. The higher-sensitivity version, with climate sensitivity of 6.3 K for doubled CO₂ forcing, overestimates cooling due to the volcanic eruption, whereas the lower-sensitivity version (4.0 K) produces results consistent with observations. The difference between the two versions is attributed to feedback processes related to clouds. This validation method is expected to provide additional constraints on climate sensitivity and may lead to reduced uncertainties in climate prediction.

Statement of the main point

The likelihood of climate sensitivity is tested by simulating global volcanic cooling after a large volcanic eruption using two versions of a coupled atmosphere-ocean general circulation model with climate sensitivities of 4.0 K and 6.3 K. The cooling predicted by the higher-sensitivity version is too large to explain the observations, whereas the lower-sensitivity version produces realistic results. This difference is attributed to a feedback process related to clouds.

Relation to previous work

No studies have attempted to simulate volcanic cooling using a general circulation model in order to test the likelihood of climate sensitivity, although the water vapor feedback has been tested by this approach. Previous attempts to constrain the climate sensitivity based on the mean present-day climate or 20th Century warming trend have been unable to reject the possibility of high sensitivities (6 K). This work presents a method that allows the sensitivity to be effectively constrained to lower values. A simple and novel feedback scheme is devised for diagnosing the strength of various climate feedbacks from the conventional model output.

Climate sensitivity, defined in the present study as the equilibrium response of global mean surface air temperature to doubling of the atmospheric CO₂ concentration, is one of the most important features of numerical models for future climate projection (1). However, as the climate sensitivity measured by climate models includes a substantial degree of uncertainty (the Intergovernmental Panel on Climate Change; 1, 2), it is crucial to reduce the uncertainty in predictions in order to accurately assess future global warming. Reducing this uncertainty by simply testing a model's ability to simulate the mean present-day climate is difficult. Recently, numerical experiments conducted using a general circulation model (GCM) with a multi-thousand-member ensemble have shown that the climate sensitivity may be anywhere from 2 K to 11 K (3). The models indicating sensitivities at the high end cannot be rejected, as the multi-year mean control climate of these models has good fidelity with observations (3).

Climate sensitivity can also be tested by comparison of modeled and observed historical climate changes. Such comparisons consider climate changes on the time scale of multiple years, such as global cooling after large volcanic eruptions (4, 5), or on much longer time scales, such as the global warming trend in the late twentieth century (6-8). As the latter includes appreciable uncertainty, mainly related to historical forcing (5), the results tend to accept the possibility of high sensitivities (6 K or higher). Studies on shorter time scales (4, 5) have employed simple energy balance models, and thus have been unable to consider cloud processes explicitly, which are expected to play a key role in determining climate sensitivity (9). Simulations of volcanic cooling using GCMs as a test of climate sensitivity have not been considered to date (10). In this study, this approach is adopted for simulation of the climate response to the volcanic eruptions of Mount Pinatubo in the Philippines in 1991, the forcing and response for which were well observed (11, 12). Two versions of a coupled atmosphere-ocean GCM (13, 14) with different climate sensitivities are considered, and the validity of the climate sensitivities indicated by these versions is examined by comparison with the observed response to the Pinatubo eruptions.

The climate sensitivities of the two versions of the model (*15, 16*) are 4.0 K (lower-sensitivity, LS) and 6.3 K (higher-sensitivity, HS). The LS and HS versions differ only in the treatment of clouds (*17*). The LS and HS versions both provide realistic simulations of the mean present-day climate, with climate prediction indices (CPIs), an objective measure of reliability (*18*), of 5.62 and 5.66, respectively (*19*).

The Pinatubo experiment consists of control and perturbed sets of ensemble runs of the coupled GCM. The control run was integrated under the preindustrial (1850) condition for more than 600 years without a significant trend of warming or cooling in the atmosphere or ocean. The perturbed runs were performed for a period of 10 years with volcanic forcing based on the stratospheric aerosol optical thickness at 550 nm (*12*) imposed on the control condition. Four-member-ensemble runs were performed using different initial conditions picked from the control run.

The time series of globally averaged surface air temperature (SAT) in the Pinatubo experiments is shown in Fig. 1. Both versions indicate cooling after the volcanic eruption. Compared to the HS version, the LS version exhibits less cooling and a shorter recovery time. This result is consistent with that of the doubled CO₂ experiments, in which the LS version has smaller SAT response. The difference between the LS and HS versions becomes larger than the ensemble standard deviations approximately two years after the eruption.

The ensemble means of the two versions of the model are compared to the observed SAT change (*20*) in Fig. 1. The time series of the observed data with the El Niño Southern Oscillation (ENSO) signal removed is also shown (*21*). Compared to the HS version, the LS version shows better agreement with the observations. The time series of the observation (both with and without the ENSO signal) settle almost within the range of the ensemble standard deviation of the LS version, but not for the HS version. This result suggests that HS version fails to explain the observations satisfactorily.

Note that the SAT response discussed above depends not only on the climate sensitivity of the model, but also on the nature of the radiative forcing imposed on the model. The observed estimate of the solar radiation anomaly at the top of the atmosphere (TOA) after the Pinatubo eruption is well reproduced by both the LS and HS versions (22). It has also been confirmed that the radiative forcings by these two versions are almost identical (less than 0.1 Wm^{-2} difference) and are consistent with the estimation by Hansen *et al.* (12, 23).

By constructing a simple scheme for diagnosis of the strength of climate feedback from the conventional model output, the mechanism responsible for the dissimilar responses of the LS and HS versions is investigated. Among the many feedback diagnoses developed to date (9, 24, 25), the present scheme is particularly useful in that it allows for a gross evaluation of major feedback processes from a straightforward calculation. By performing feedback analysis on the doubled CO_2 experiment which has also been used to measure climate sensitivity (16) as well as the Pinatubo experiment, the similarities and differences between the LS and HS versions in the two experiments are examined, and the validity of applying constraints on the climate sensitivity based on the Pinatubo experiment is discussed.

The strength of the feedback processes is evaluated from anomalies in the solar radiation (shortwave radiation, SW) and terrestrial radiation (longwave radiation, LW) fluxes at the TOA. The anomalies are calculated by the difference between the perturbed and control runs for the Pinatubo and doubled CO_2 experiments. By breaking down the SW and LW flux anomaly at the TOA into contributions from the surface, clear-sky atmosphere (defined as the part of the atmosphere except clouds), and clouds, we evaluate ice-albedo feedback (the SW flux anomaly owing to changes in the area or radiative properties of ices at the surface), cloud feedback (the SW and LW flux anomaly owing to changes in the amount or radiative property of clouds), Stefan-Boltzmann feedback (the LW flux anomaly owing to changes in the surface temperature), and combined water vapor and lapse rate feedback (LW flux anomaly owing to changes in

the properties of clear-sky atmosphere, such as water vapor amount or vertical atmospheric temperature profile). Responses due to feedback processes are computed by subtracting the radiative forcing component from the anomalies in the SW and LW fluxes. Then, the feedback parameters are calculated by dividing the global mean of the responses by that of the SAT anomaly (17).

The feedback parameters in the Pinatubo and doubled CO₂ experiments are shown in Fig. 2. Positive feedback parameters indicate enhancement of cooling in the Pinatubo experiment, and enhancement of warming in the doubled CO₂ experiment. Both experiments show that the strongest feedback factors are the Stefan-Boltzmann feedback (SFC-LW), the water vapor and lapse rate feedback (CLR-LW), and the cloud albedo feedback (CLD-SW). The other factors are relatively minor.

The feedback parameters for SFC-LW and CLR-LW are similar in the Pinatubo and doubled CO₂ experiments, despite the dissimilar nature of forcing and the time scale of the response. The feedback parameter for CLD-SW is negative in the Pinatubo experiment, yet positive in the doubled CO₂ experiment. This difference in sign can be attributed to the latitudinal distribution of forcing. The negative feedback over the tropics works effectively in the Pinatubo experiment because the volcanic forcing centered on the tropics reduces convection and the formation of anvil clouds. In the doubled CO₂ experiment, on the other hand, the signal of cloud reduction over the subtropics overwhelms that of cloud increase in the tropics, leading to a positive parameter for CLD-SW.

In both the Pinatubo and doubled CO₂ experiments, the maximum difference in the feedback parameters between the two versions of the model occurs in CLD-SW. This difference can be attributed to the cloud response at the mid-to-high latitudes, where the LS version produces stronger negative feedback than the HS version in both experiments. This result is consistent with that of Ogura *et al.* (16), who conducted a detailed analysis of the cloud response to

doubled CO₂ forcing using the two versions of this model.

The cloud-albedo feedback in the LS and HS versions can be validated by calculating the SW flux anomaly due to clouds ($\Delta F_{\text{cld}}^{\text{sw}}$, positive defined as downward direction) following the Pinatubo eruption using the radiative flux estimates determined from the globally observed data set, ISCCP-FD (26, 27). In the ISCCP-FD data, $\Delta F_{\text{cld}}^{\text{sw}}$ is 0.58 Wm^{-2} , where this anomaly of SW flux is $0.77 \pm 0.19 \text{ Wm}^{-2}$ in the LS version and $0.36 \pm 0.33 \text{ Wm}^{-2}$ in the HS version (the \pm refers to the ensemble standard deviation). Considering the suspected overestimate of the SW reflection by clouds (i.e. underestimate of $\Delta F_{\text{cld}}^{\text{sw}}$) following the Pinatubo eruption in the ISCCP-FD data (26), the $\Delta F_{\text{cld}}^{\text{sw}}$ produced by the LS version appears to be closer to reality.

On the basis of this feedback analysis, the difference in the global mean SAT response between the LS and HS versions appears to originate mainly from the cloud-albedo feedback, in both the Pinatubo and doubled CO₂ experiments. Although the sign in the cloud-albedo feedback differs between the two experiments (negative in Pinatubo and positive in doubled CO₂), the HS version consistently produces a more positive feedback than the LS version in the two experiments (smaller negative in Pinatubo and larger positive in doubled CO₂). As the factor that determines the difference between the LS and HS versions in the Pinatubo and doubled CO₂ experiments is the same (i.e., cloud-albedo feedback), the reliability of the LS and HS versions in the doubled CO₂ experiment can be reasonably tested by the results of the Pinatubo experiment.

The global mean SAT response of the LS version to the Pinatubo forcing is in better agreement with the observations than the HS version. The cloud-albedo feedback of the LS version after the Pinatubo eruption is also likely to be more consistent with the observations. Therefore, the climate response of the LS version is considered to be more reliable, and thus the climate sensitivity of the LS version (4.0 K) is expected to be more reasonable than that of the HS version (6.3 K).

The climate sensitivity could differ among climate models for various reasons, not necessarily due solely to differences in the cloud-albedo feedback. Therefore, the present results should only be valid for models in which the climate sensitivity is strongly dependent on the cloud-albedo feedback. However, the present work demonstrates that it is possible to test the likelihood of climate sensitivity by hindcasting the response to a volcanic eruption. As the feedback analysis used in this work can be readily applied to the conventional output of other GCMs, the same tests should be performed for other models. This validation method for climate models is therefore expected to improve our understanding of the uncertainty in climate sensitivity, which may be of great use in projecting the possible range of future climate changes.

References and Notes

1. U. Cubasch *et al.*, in *Climate Change 2001: The Scientific Basis*, J. T. Houghton *et al.* Eds., (Cambridge Univ. Press, Cambridge, 2001) 525-582pp.
2. B. J. McAvaney *et al.*, in *Climate Change 2001: The Scientific Basis*, J. T. Houghton *et al.* Eds., (Cambridge Univ. Press, Cambridge, 2001) 471-523pp.
3. D. A. Stainforth *et al.*, *Nature* **433**, 403 (2005).
4. R. S. Lindzen, C. Giannitsis, *J. Geophys. Res.* **103**, 5929 (1998).
5. T. M. L. Wigley *et al.*, submitted to *J. Climate* (2005).
6. N. G. Andronova, M. E. Schlesinger, *J. Geophys. Res.* **106**, 22605 (2001).
7. C. E. Forest *et al.*, *Science* **295**, 113 (2002).
8. R. Knutti *et al.*, *Nature* **416**, 719 (2002).
9. R. D. Cess *et al.*, *J. Geophys. Res.* **95**, 16601 (1990).

10. Although the effects of water vapor feedback have been studied by volcanic cooling simulations using GCMs (28, 29), feedback processes related to clouds, which are some of the most important factors in determining climate sensitivity, have not been examined to date.
11. A. Robock, *Rev. Geophys.* **38**, 191 (2000)
12. J. Hansen *et al.*, *J. Geophys. Res.* **107**, 4373, doi:10.1029/2001JD001143 (2002).
13. K-1 model developers, “K-1 coupled GCM (MIROC) description” (K-1 Tec. Rep. 1, Univ. of Tokyo, Tokyo, 2004).
14. The atmospheric component of the model has a horizontal resolution of approximately 2.8° latitude by 2.8° longitude (spectral resolution with triangular truncation at wavenumber 42) with 20 levels, and the ocean component has a horizontal resolution of 1.4° latitude by 1.4° longitude with 43 levels.
15. The climate sensitivities of the two versions of the model were measured by performing the doubled CO₂ experiment using the atmospheric part of the coupled GCM with a mixed-layer ocean model in which ocean heat transport is prescribed (16). The control run with the preindustrial condition (285 ppm CO₂) and the perturbed run with the condition of doubled atmospheric CO₂ concentration (570 ppm) were performed until equilibrated states of the atmosphere were achieved.
16. T. Ogura *et al.*, in preparation (2005).
17. Details of the methods are available as supporting material on *Science Online*.
18. J. M. Murphy *et al.*, *Nature* **430**, 768 (2004).

19. The cloud components of the CPI were calculated by masking out clouds over the ocean at high latitude ($> 50^\circ$). It has further been confirmed that the distributions of clouds over those area in the LS and HS versions are also similar.
20. P. D. Jones, A. Moberg, *J. Climate* **16**, 206 (2003).
21. The ENSO signal in the observations was removed by the method of Santer *et al.* (30). It was not removed from the simulated time series because it should be canceled, to some extent, in the ensemble mean. The ENSO signal cannot be properly removed by Santer's method in the latter case because the model ENSO signal is so weak that the volcanic signal is projected to the modeled ENSO index.
22. The solar radiation anomalies at the TOA in the LS and HS versions was calculated in the same way as shown in Fig. 6a of Zhang *et al.* (26). It was confirmed that the modeled anomaly is within the range of uncertainty in the observations.
23. Although other estimates of the radiative forcing for the Pinatubo event have been reported (31, 32), these alternative estimates are generally larger than the forcing imposed in the present work. Thus, the better agreement of the LS version with the observations and the inability of the HS version to explain the observations satisfactorily would not change even if higher estimates of forcing were employed.
24. R. T. Wetherald, S. Manabe, *J. Atmos. Sci.* **45**, 1397 (1988).
25. G. J. Boer, and B. Yu, *Clim. Dyn.* **20**, 415 (2003).
26. Y. Zhang *et al.*, *J. Geophys. Res.* **109**, D19105, doi:10.1029/2003JD004457 (2004)

27. Even though the ISCCP-FD data contains uncertainty of $5\text{--}10 \text{ Wm}^{-2}$, the data is in good agreement with the Earth Radiation Budget Satellite (ERBS) data (26). The observed and modeled value of $\Delta F_{\text{cld}}^{\text{sw}}$ are calculated based on the difference between time-averaged values taken 1–3 yr after the eruption and that 1 yr before the eruption. Linear trend from 1981 to 2000 is removed from the observed value.
28. B. J. Soden *et al.*, *Science* **296**, 727 (2002).
29. P. M. de F. Foster, M. Collins, *Clim. Dyn.* **23**, 207 (2004).
30. B. D. Santer *et al.*, *J. Geophys. Res.* **106**, No. D22, 28033-28059 (2001).
31. G. L. Stenchikov *et al.*, *J. Geophys. Res.* **103**, 13837 (1998).
32. N. G. Andronova *et al.*, *J. Geophys. Res.* **104**, 16807 (1999).
33. The authors thank Akimasa Sumi, Hideo Shiogama, Tatsuya Nagashima, Naosuke Okada for valuable discussion and encouragement. We acknowledge David Sexton for CPI calculations. This work was supported as the Kyousei project promoted by the Ministry of Education, Culture, Sports, Science and Technology of Japan. Model calculations were made on an NEC SX-6 supercomputer at NIES and the Earth Simulator.

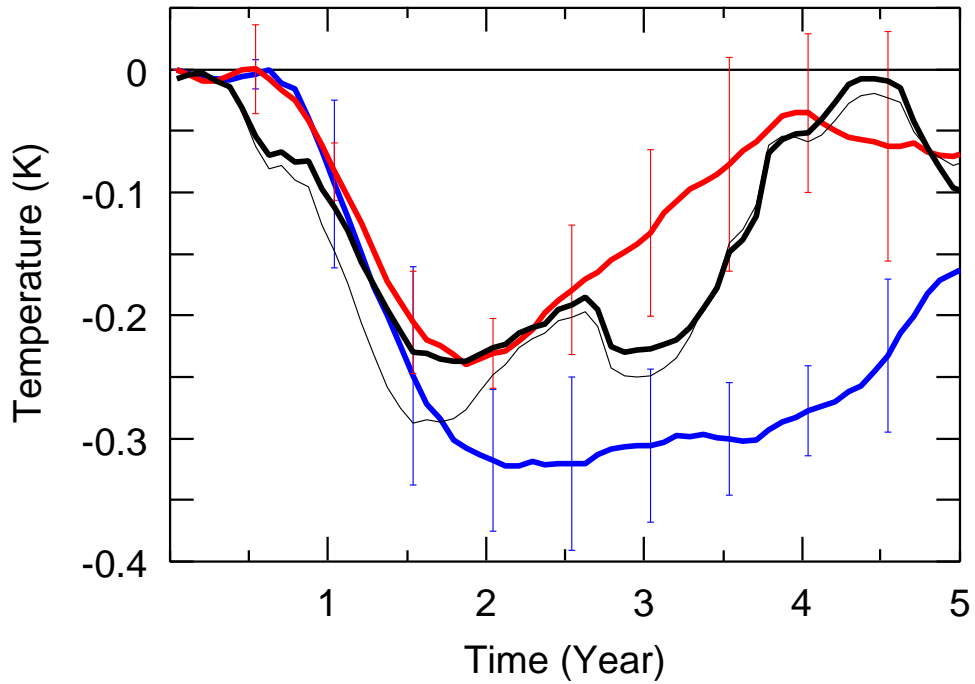


Fig. 1: Anomaly time series of global mean surface air temperature (SAT) after the Pinatubo volcanic eruption simulated by model versions with climate sensitivity of 4.0 K (LS, red) and 6.3 K (HS, blue). SAT observations by HadCRUT2v (20) with the linear trend from 1981 to 2000 removed (thick black) and that with the ENSO signal additionally removed (thin black) by the method of Santer *et al.* (30) are also shown. Modeled and observed anomalies are calculated by taking the mean of 12 months prior to the eruption as a baseline. The global mean was computed by taking the area-weighted average in the region where observational data are available. The time series are smoothed by a 12-month moving average, and error bars denote the standard deviation of the model ensembles.

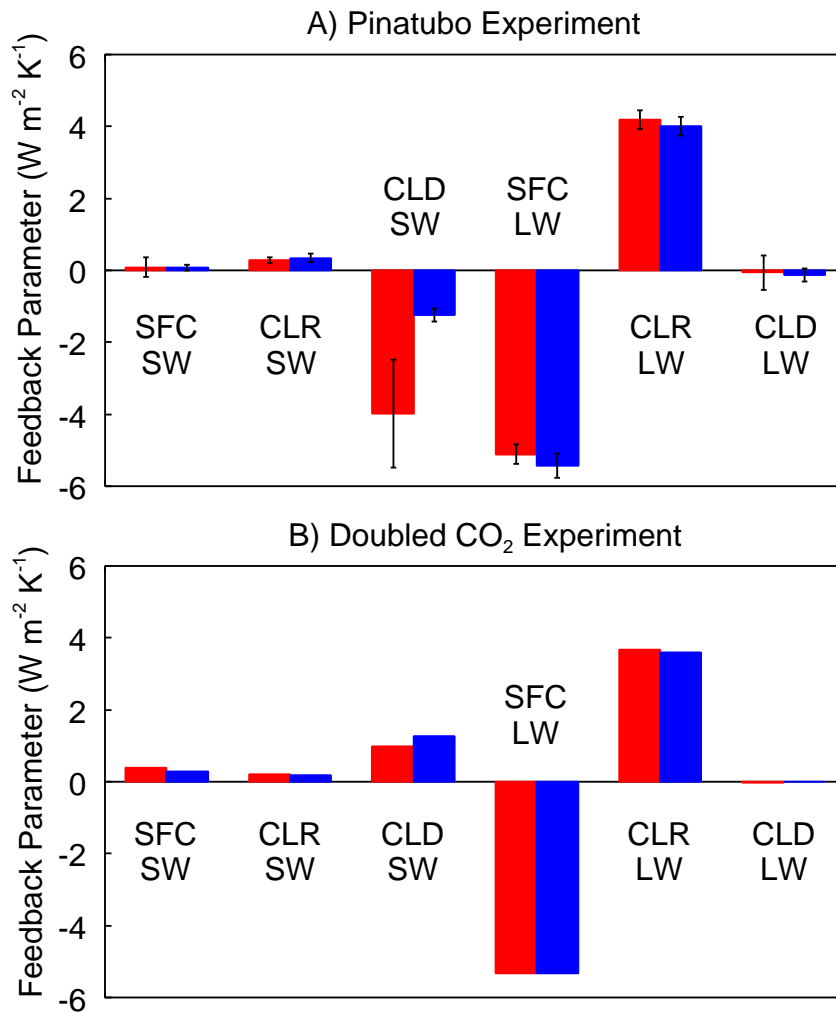


Fig. 2: Feedback parameters for the (A) Pinatubo experiment and (B) doubled CO₂ experiment, showing results for the LS (red) and HS (blue) versions of the model. Bars represent the feedback parameters for the SW flux anomalies due to the surface (SFC-SW), clear-sky atmosphere (CLR-SW), and clouds (CLD-SW), and the LW flux anomalies due to the surface (SFC-LW), clear-sky atmosphere (CLR-LW), and clouds (CLD-LW). Anomalies were calculated by (A) the difference between time-averaged values taken 1–3 yr after the eruption and that 1 yr before eruption, and (B) by the difference between the equilibrated states of the perturbed and control runs. Error bars denote the standard deviations of the model ensembles.

Supporting Online Material

Climate response to volcanic forcing: Validation of climate sensitivity of a coupled atmosphere-ocean general circulation model

Tokuta Yokohata,^{1*} Seita Emori,^{1,2} Toru Nozawa¹
Yoko Tsushima², Tomo'o Ogura¹ and Masahide Kimoto³

¹National Institute for Environmental Studies

²Frontier Research Center for Global Change

²Center for Climate System Research

Description of general circulation model

The coupled atmosphere-ocean general circulation model employed is MIROC version 3.2 (*I*), which was developed cooperatively by the Center for Climate System Research (CCSR) of the University of Tokyo, the National Institute for Environmental Studies (NIES), and the Frontier Research Center for Global Change (FRCGC) of the Japan Agency for Marine-Earth Science and Technology.

The difference in cloud treatment between the lower-sensitivity (LS) version and higher-sensitivity (HS) version is formulated in terms of large-scale condensation (2) as follows. 1) Liquid and solid phases of cloud water coexists between 258 K and 273 K in the LS version, and between 248 K and 268 K in the HS version. 2) Melted cloud ice falls to the ground instantaneously in the LS version, yet remains suspended in the air as cloud liquid water in the HS version. The formulations of the LS and HS versions are both within the range of uncertainty in the model parameterization.

Simple feedback analysis scheme

A simple scheme was devised to diagnose major feedback processes from the conventional model output. The feedback parameters is calculated as follows. 1) Anomaly in net SW flux at the TOA is broken down into contributions from the surface, ($\Delta F_{\text{sfc}}^{\text{sw}}$), clear-sky atmosphere ($\Delta F_{\text{clr}}^{\text{sw}}$), and clouds ($\Delta F_{\text{cld}}^{\text{sw}}$). Here, clear-sky atmosphere is defined as the part of the atmosphere except clouds. 2) Anomaly in net LW flux at the TOA is also broken down into the three components ($\Delta F_{\text{sfc}}^{\text{lw}}$, $\Delta F_{\text{clr}}^{\text{lw}}$ and $\Delta F_{\text{cld}}^{\text{lw}}$). 3) Instantaneous SW and LW radiative forcing at the TOA are calculated and broken down into the three components (ΔG_i^j , $i = \text{sfc, clr, cld}$ and $j = \text{sw, lw}$). 4) Responses due to feedback processes are calculated by subtracting the forcing component from the anomalies in the net SW and LW fluxes ($\Delta R_i^j = \Delta F_i^j - \Delta G_i^j$). 5) The feedback parameters are calculated by dividing the global mean of the responses (ΔR_i^j) by that of the SAT anomaly (ΔT_s). The ice-albedo feedback can then be evaluated by $\Delta R_{\text{sfc}}^{\text{sw}}/\Delta T_s$, the cloud feedback by $\Delta R_{\text{cld}}^{\text{sw}}/\Delta T_s$ and $\Delta R_{\text{cld}}^{\text{lw}}/\Delta T_s$, the Stefan-Boltzmann feedback by $\Delta R_{\text{sfc}}^{\text{lw}}/\Delta T_s$, and the combined water vapor and lapse rate feedback by $\Delta R_{\text{clr}}^{\text{lw}}/\Delta T_s$. The details of above procedure from 1) to 3) are as follows.

1) Breaking down the SW flux anomaly at the TOA

The method to break down the anomaly in the net SW flux at the TOA into contributions from the surface, the clear-sky atmosphere and clouds is as follows. First, the net SW flux at the TOA of the model output ($F_{\text{toa}}^{\text{sw}}$, positive defined as downward direction) is divided into contributions from the surface and the full-sky atmosphere, as shown in Fig. S1 and expressed as

$$F_{\text{toa}}^{\text{sw}} = F_0 - A_{\text{sfc}} T_{\text{ful}}^2 F_0 - A_{\text{ful}} F_0, \quad (\text{S1})$$

where A and T denote the albedo and transmissivity of the surface (sfc) and full-sky atmosphere (ful), and F_0 is the downward SW flux at the TOA (3). As the variables in Eq. (S1) other than A_{ful} can be obtained from the conventional model output (A_{sfc} by the ratio between the upward and downward SW flux at the surface, T_{ful} by the ratio between the full-sky downward SW flux at the TOA and the surface), it is possible to find A_{ful} in the perturbed and control runs. The clear-sky values A_{clr} and T_{clr} can also be found by formulating the clear-sky net SW flux at the TOA in the same way as Eq. (S1).

The albedo and transmissivity of the full-sky atmosphere (A_{ful} and T_{ful}) can then be presented as functions of clear-sky atmosphere (A_{clr} and T_{clr}) and cloudy (A_{cld} and T_{cld}) values. For this purpose, a simple two-layer model is assumed (4), as shown in Fig. S1 and described by

$$A_{\text{ful}} = A_{\text{clr}} + (1 - A_{\text{clr}})A_{\text{cld}} \quad (\text{S2})$$

$$T_{\text{ful}} = T_{\text{clr}}T_{\text{cld}} \quad (\text{S3})$$

A_{cld} and T_{cld} can be derived from Eqs. (S2) and (S3) in the perturbed and control runs. By substituting Eqs. (S2) and (S3) into Eq. (S1) and obtaining the perturbation, the anomaly in $F_{\text{toa}}^{\text{sw}}$ can be calculated as follows.

$$\begin{aligned} \Delta F_{\text{toa}}^{\text{sw}} = & -\Delta A_{\text{s}}(T_{\text{clr}}T_{\text{cld}})^2 F_0 \\ & -2T_{\text{clr}}\Delta T_{\text{clr}}(A_{\text{sfc}}T_{\text{cld}}^2)F_0 - (1 - A_{\text{cld}})\Delta A_{\text{clr}}F_0 \\ & -2T_{\text{cld}}\Delta T_{\text{cld}}(A_{\text{sfc}}T_{\text{clr}}^2)F_0 - (1 - A_{\text{clr}})\Delta A_{\text{cld}}F_0, \end{aligned} \quad (\text{S4})$$

where Δ denotes the difference between the perturbed and control runs, and the other values are those of the control run. The term on the first line of Eq. (S4) is regarded as the contribution from the surface ($\Delta F_{\text{sfc}}^{\text{sw}}$), those on the second line represent the clear-sky-atmosphere contribution

($\Delta F_{\text{clr}}^{\text{sw}}$), and those on the third line are the cloud contribution ($\Delta F_{\text{cld}}^{\text{sw}}$).

2) Breaking down the LW flux anomaly at the TOA

The TOA LW flux is not broken down in the same way as the SW flux because the LW flux contains components of emission as well as absorption, and thus the nature of LW flux at the TOA is essentially different from that of the SW flux. Instead, the surface contribution to the anomaly in the net LW flux ($\Delta F_{\text{sfc}}^{\text{lw}}$, positive downward) is formulated as the conventional Stefan-Boltzmann feedback (e.g., 5), which is calculated by the anomaly in the upward LW flux at the surface. The clear-sky atmospheric contribution ($\Delta F_{\text{clr}}^{\text{lw}}$) is formulated as the atmospheric greenhouse effect (e.g., 6), and is calculated by the anomaly in the difference between the upward LW flux at the surface and the clear-sky upward LW flux at the TOA. The contribution from clouds ($\Delta F_{\text{cld}}^{\text{lw}}$) is formulated as the conventional cloud radiative forcing (e.g. 7), and is calculated by the anomaly in the difference between the clear-sky and full-sky upward LW fluxes at the TOA.

3) Calculating and breaking down the radiative forcing

The instantaneous radiative forcing is calculated by calling the radiation code twice in the control runs of the Pinatubo and doubled CO₂ experiments. In one call, the forcing variable (Pinatubo volcanic aerosol or doubled CO₂ concentration) is set to the control value, and in the second call, it is set to the perturbed value. The radiative forcing is calculated as the difference in the net SW and LW radiative fluxes at the TOA between the two calls. The SW and LW radiative forcing are then broken down into contributions from the surface, clear-sky atmosphere and clouds in the same way as described above.

References and Notes

1. K-1 model developers, “K-1 coupled GCM (MIROC) description” (K-1 Tec. Rep. 1, Univ. of Tokyo, Tokyo, 2004).
2. T. Ogura *et al.*, in preparation (2005).
3. The formulations of Eq. (S1) are essentially the same as those determined by Qu and Hall (8), but assuming the ratio of the atmospheric transmissivity to downward and upward SW flux to be unity for simplicity. It has been confirmed that this is a fair approximation based on calculations of radiative fluxes using a surface albedo of zero.
4. The two-layer formulation was adopted because the aim is to represent the TOA SW flux as a simple function of the surface, clear-sky atmosphere and clouds. Absorption and multiple-scattering by the scattering agents are neglected for simplicity, but it has been confirmed that the former is negligible and that the latter may cause only a small error. Note that this formulation is not dependent on the vertical order of the two scattering agents, and thus can be applied to the Pinatubo and doubled CO₂ experiments even though the vertical structures of the major scattering agent differ (stratospheric volcanic aerosols exist above the clouds in the Pinatubo experiment, tropospheric aerosols exist below the clouds in the doubled CO₂ experiment).
5. D. L. Hartmann, *Global physical climatology*, (Academic Press, San Diego, 1994), pp.229-253.
6. G. A. Meehl *et al.*, *J. Climate* **17**, 1584 (2004).
7. T. P. Charlock, V. Ramanathan, *J. Atmos. Sci.* **42**, 1408 (1985).
8. X. Qu, A. Hall, submitted to *J. Climate* (2005).

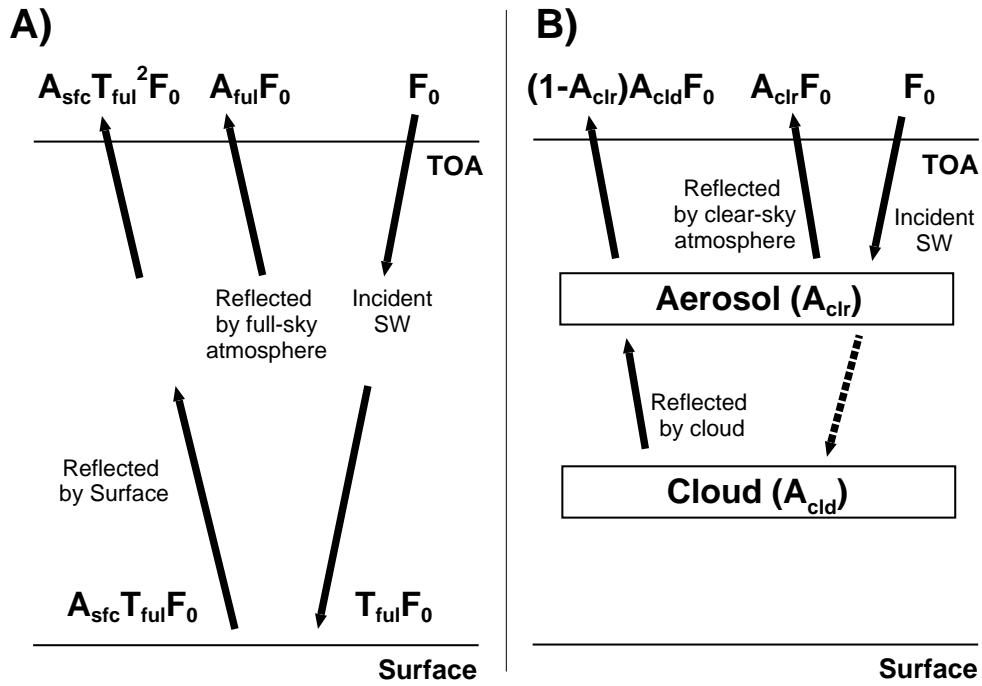


Fig. S1: (A) Formulation for breaking down the SW flux at the TOA into contributions from the surface and full-sky atmosphere. A and T denote the albedo and transmissivity of the surface (sfc) and full-sky atmosphere (ful), and F_0 is the downward SW flux at the TOA. The ratio of the atmospheric transmissivity to the downward and upward SW flux is assumed to be unity. (B) Relationship between the SW albedo of the full-sky and that of the clear-sky atmosphere (clr) and cloud (cld) based on a simple two-layer model.